Kinematical characteristic of mechanical frictional variable speed drive

D. Herák[1], V. Šleger[1], R. Chotěborský[2], K. Houška[3], E. Jančа[1]

[1]*Department of Mechanics and Engineering, Technical Faculty, Czech University of Agriculture in Prague, Prague, Czech Republic*
[2]*Department of Material and Engineering Technology, Technical Faculty, Czech University of Agriculture in Prague, Prague, Czech Republic*
[3]*HouseMax International, Ltd., Prague, Czech Republic*

Abstract: The paper describes a new system of mechanical spherical conical friction drive. In the present a row of simple friction, belt, chain, wave and differential variable speed drives is published. For the required range of speed variation they are altogether unfit. The currently used power transmissions are of low efficiency (60–70%). Therefore the better power transmission efficiency is required. The possibility of multicontact power transmission appears as the most suitable principle of the power transmission. Using the designed function model, which was made according to the small tractor producers requirements, the real output kinematical characteristic was measured. It is derived the complete drive conversion unit kinematics and the theoretical kinematical characteristic design. The theoretical design is compared with the real characteristic determined by measuring using the test station. From the measured values we determined that the geometrical characteristic, i.e. the relation between output speed and ring position, corresponds in the ring position range (2.8÷14) mm to the theoretical premise.

Keywords: variable speed drive; friction drive; kinematical characteristic; kinematical design

The transmission of power from the drive motor to the travel wheel of a road or rail vehicle does not dispense with a transmission mechanism, which can be designed by a simple one-stage mechanical gear transmission as at the electric drive of a rail vehicle axle up to a complicated gear of a commercial vehicle, passenger car or bus, which contains a combination of a hydraulic and mechanical drive and a complicated automatic control (Kopáček 1997).

In practice mechanical variable speed drives are often used. They are transmission mechanisms with a stepless drive ratio. Speed drives field of application is very different reaching from medical instruments to heavy presses in scrap yards. The stepless drive ratio makes possible the optimization of the machine capacity at a given load. For powers to 50 kW the classical mechanical speed drives are noted for a small control range, which does not correspond to requirements of producers of small tractors, passenger cars and other mobile engineering (Zachariáš 2005).

Therefore the Czech tractor producers clamour for a mechanical variable speed drives development for almost 10 years due to their law efficiency (65–75%). Today this efficiency is reached using hydrostatical drives or expensive and complicated multispeed gearboxes. Moreover the conversion of mechanical energy to other energy type – pressure head or electric energy – heightens the capital assets of otherwise simple machine and generally decreases the operating reliability of small tractors. The variable speed drives using pulleys with adjustable sheaves assign a low pulleys service life and significantly decrease the operating costs.

Therefore the low efficiency of currently used power transmissions causes the requirement of the motor better energy utilization.

Designed variable speed drive

A row of variable speed drives using friction, belts, chains etc. which are unsuitable for the demanded speed range has been published (Bolek & Kochman 1989, 1990; Švec 1999).

Consumers are interested in small tractors, mobile pavement cleaners and little snow-plough carriers

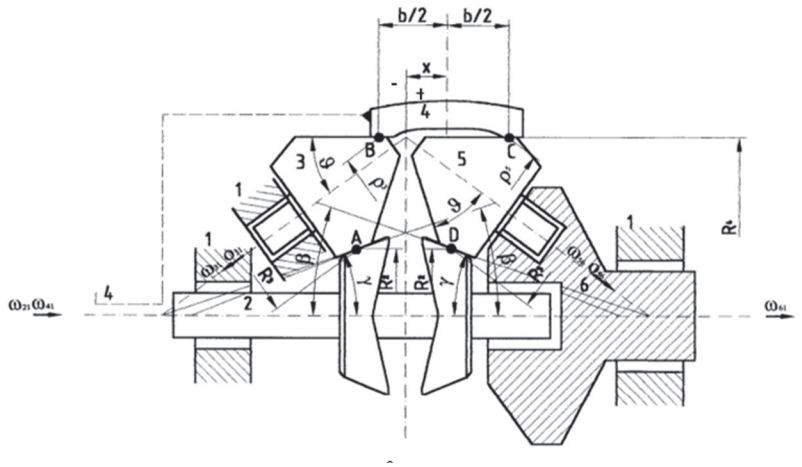

Figure 1. Kinematical diagram of the variable speed drive

with a petrol engine of 4 to 10 kW power. Therefore producers accept this demand and rather buy suitable four-stroke engines from various producers, e.g. Honda motor, P = 4 kW at revolutions n = 3750 1/min.

The use of the friction multi-contact power transmission appears as the most useful (Zachariáš 2005).

In collaboration with an industrial enterprise the friction planetary infinitely variable speed drive was designed in our department. It fulfils all theoretical conditions of the optimal working.

The frictional spherical planetary speed drive is arranged according to the kinematical diagram in Figure 1. It is fitted with a system of five cones 3 located on fixed axes and with a system of five cones 5, which create the planet wheels.

The input shaft 2 rotates with a constant speed and the output shaft rotates with various speeds, which depend on the displacement of the ring 4. By the displacement of the ring 4 we get the stepless variable speeds.

For the contact forces adjustment on the abscissas and in the places A, B, C, D the ring 4 is arranged as the close coupling which is created by the parted sleeve with the pair of outer sleeves planted with screws.

The displacement of the ring 4 is realized by means of the motion screw. The input shaft of the motion screw is controlled by means of a speed governor (Herák 2005).

Kinematical solution of the variable speed drive

Analysis of the transmission elements

The choice of the rolling points and angular velocity vectors is shown in Figure 1.

$\mathbf{A} \equiv \mathbf{P}_{\mathbf{32}}$ Analysis of motion 31 = 32 + 21

$$\omega_{31} \times R_3 = \omega_{21} \times R_2 \quad (1)$$

$\mathbf{B} \equiv \mathbf{P}_{\mathbf{34}}$ Analysis of motion 31= 34 + 41

$$\omega_{31} \times \rho_3 = -\omega_{41} \times R_4 \quad (2)$$

$\mathbf{C} \equiv \mathbf{P}_{\mathbf{54}}$ Analysis of motion 51 = 56 + 61, resp. 51 = 54 + 41 ($v_{51} = v_{41}$)

$$\omega_{41} \times R_4 = \omega_{56} \times \rho_5 + \omega_{61} \times R_4 \quad (3)$$

$\mathbf{D} \equiv \mathbf{P}_{\mathbf{52}}$ Analysis of motion 51 = 56 + 61, resp. 51 = 52 + 21 ($v_{51} = v_{52}$)

$$\omega_{21} \times R_2 = -\omega_{56} \times R_5 + \omega_{61} \times R_4 \quad (4)$$

Expression of ρ_3, ρ_5 radiuses (Figure 1)

$$\rho_3 = \left(\frac{b}{2} - x\right) \times \sin \vartheta$$

$$\rho_5 = \left(\frac{b}{2} - x\right) \times \sin \vartheta$$

The angular velocities are directly proportional to the revolutions,

$$\omega = \frac{\pi \times n}{30}$$

where: n (min).

According to the equation (1) the constant revolutions are

$$n_{31} = \frac{R_2}{R_3} \times n_{21} \quad (5)$$

According to the equation (2) it is true

$$n_{41} = \frac{-\rho_3}{R_3} \times n_{31} = -n_{21} \times \frac{R_2}{R_3 \times R_4} \times \left(\frac{b}{2} - x\right) \times \sin \vartheta \quad (6)$$

The ring 4 revolutions vary with the change of x.

The ring rotates reverse to the drive shaft 2.

We multiply the equation (3) by R_5, the equation (4) by ρ_5 and we add both equations. Then we get

$$n_{41} \times R_4 \times R_5 + n_{21} \times R_2 \times \rho_5 = n_{61} \times (R_4 \times R_5 + R_2 \times \rho_5)$$

After substitution for n_{41}

$$n_{21} \times \left(-\frac{R_2 \times R_5}{R_3} \times \rho_3 + R_2 \times \rho_5 \right) = n_{61} \times (R_4 \ R_5 + R_2 \times \rho_5)$$

From here the total drive ratio of the variable-speed drive at $R_3 = R_5$

$$\frac{n_{61}}{n_{21}} = \frac{R_2 \times \left(\rho_5 - \frac{R_5}{R_3} \times \rho_3 \right)}{R_2 \times \left(\rho_5 + \frac{R_4 \times R_5}{R_2} \right)} = \frac{2 \times x \times \sin\vartheta}{x \times \sin\vartheta + \frac{b}{2} \times \sin\vartheta + \frac{R_4 \times R_5}{R_2}} =$$

$$= \frac{2 \times x}{x + \frac{b}{2} + \frac{R_4 \times R_5}{R_2 \times \sin\vartheta}} \quad (7)$$

Briefly we name the summary of constant values in the denominator by the letter k.

$$k = \frac{b}{2} + \frac{R_4 \times R_5}{R_2 \times \sin\vartheta} \quad (8)$$

The total drive ratio

$$\mu_{26} = \frac{n_{61}}{n_{21}} = \frac{2 \times x}{x + k} \quad (9)$$

For completion the rotational speed of the cone set 5 with regard to the carrier 6.

From the equation (4) it follows

$$\frac{n_{56}}{n_{21}} = \frac{n_{61}}{n_{21}} \times \frac{R_2}{R_5} - \frac{R}{R_5} = \frac{R_2}{R_3} \times \left(\frac{n_{61}}{n_{21}} - 1 \right) \quad (10)$$

After the substitution for

$$\frac{n_{61}}{n_{21}}$$

from the equation (5) and after a simple adjustment we get

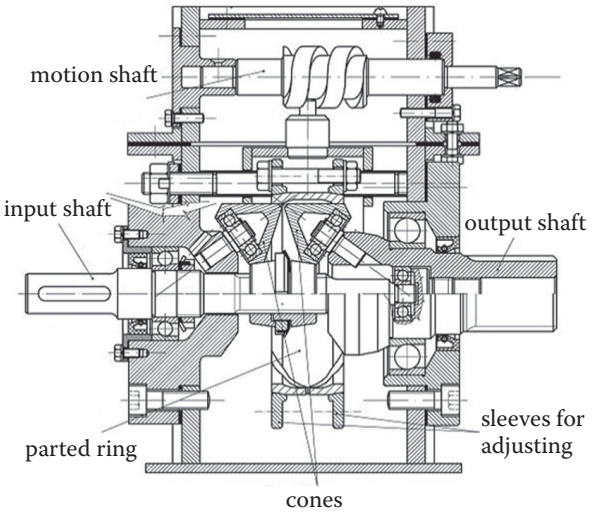

Figure 2. Gearbox section

$$n_{56} = n_{21} \times \frac{R_2}{R_5} \times \frac{x - k}{x + k} \quad (11)$$

Regarding to the fact that the constant length k is always major than the length × the rotation of the cone set 5 is of opposite direction than the presupposed direction (Figure 1) (the angular velocity ω_{56} arrow is of opposite direction).

The choice of the input shaft 2 rotational speed depends on the value of the maximum transmitted power. For the standard motors of small tractors the power of P_{max} = 4.5 kW is used and the input shaft revolutions are as a rule of n_{21} = 2920 1/min.

Except the values of power and revolutions the choice of basic sizes is required for the design.

The dimensions of the variable speed drive are following:

$R_2 = R_3 = R_5$ =18 mm
R_4 = 50 mm
$\vartheta = 36°$, $\beta = 18°$, $\gamma = 8°$

Technical arrangement

The variable speed drive is arranged in form of the two-planetary gearbox with the infinitely variable satellite diameter. The power is supplied by the input shaft, which is supported on two angular-contact ball bearings. The shaft turns the inner cones, which cause the rotation of the outer cones (Figure 2).

The outer cones near the input shaft are mounted using the angular-contact ball bearings. The bearings are pressed on the pins which are pressed on the flange. The flange is bolted on the drive housing. The outer cones near to the output shaft are mounted using bearings and pins, too. The pins are pressed on the output shaft, which is their carrier. The outer cones near to the output shaft rotate not only around their rotary axes (anyhow the cones near to the input shaft) but around the output shaft axis, too. The rotation of the outer cones near to the input causes the ring rotation. This ring causes the rotation of outer cones near to the output shaft. In this way we reach the before mentioned combined motion of the cones. The change in the satellite diameter is caused by the ring traverse (see the previous chapter).

The prestressed force, which is required for the friction force creation, is caused by the ring diameter change. The ring is designed as herring bone parted. By the adjustment of the gib screws prestressing we reach the change in the sleeves distance and in this way in the ring diameter.

The friction forces creation on the inner cones is given by their distance change. This distance is

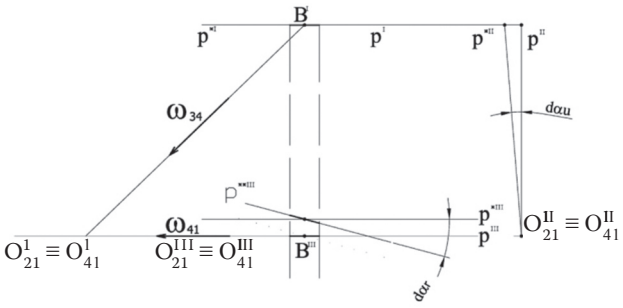

Figure 3. Graphical representation of angles of contingency

reached by the rotation of the distance nut. In this way we reach the inner cones distance change.

The ring motion is simply caused by the movable part, which is mounted on the guide rods. The part is moved by the helical groove on the shaft. By the rotation of the shaft we simply move the ring.

Geometrical arrangement of the contact line segments

With regard to the symmetry of the geometrical arrangement of the variable speed drive the geometry of the motion composition in the points B and C is the same. Therefore the tracking only of the e.g. B point is sufficient (Figure 3).

With regard to the p straight line, where the contact abscissa is in the time moment t, within the infinitesimal time dt the contact abscissa reaches the place of the straight line p^{**}, i.e. by turning through an angle of contingency $d\alpha_u$ of the motion 41.

The motion from the point p in the point p^* represents the rolling. But in the same time the turning of the straight line p through an angle of contingency $d\alpha_r$ of the relative motion 34 (dotted line, Figure 3) occurs. Because both motions – relative and carrier – run through the same time, at the end of the time interval dt the contact abscissa is on the straight line p^{**}. The angle of contingency is the angle of two infinitely impending adjoining positions. Between the positions determined by the legs of the angle of contingency no "interposition" of the contact abscisse exists. The infinitesimal angles are substituted by finite angles (Figure 4). It is possible only using the graphic illustration.

The real process is only tendentious (Figure 4). But from indicated tendencies it is evident that on the contact flat assigned to the contact straight line not only the pure rolling occurs but the combination of rolling with tendency to skidding.

Analogously on the contact flats assigned to the places A respectively D the rolling with tendency to skidding is ensured by the choice of the apex angle of the cones $\gamma = 8°$. The angle $\beta = 18°$ would correspond to the pure rolling in the places A respectively D (Faires 1955; Amiss *et al.* 2000; Král 2002).

Limiting values of revolutions for single bodies

In the previous chapter the length of the contact straight line was chosen $l = 6$ mm, the maximal effective motion of the ring $x_{max} = \pm 14$ mm at the chosen values $R_2 = R_3 = R_5 = 18$ mm, $R_4 = 50$ mm, $\vartheta = 36°$, $\beta = 18°$, $\gamma = 8°$. The premise was that in the extreme position the contact straight line will not withdraw the engagement more than by 0.5 mm. Then the dimension b, that is the distance between the points B and C, is

$$b = 2 \times x_{max} + 2 \times \frac{l}{2} = 2 \times 14 + 2 \times 3 = 34 \text{ mm} \quad (12)$$

From the equation (9) it is evident that at ring motions to $x \rightarrow 0$ the total drive ratio μ_{26} approaches to zero. Then the moment transmitted to the carrier grows beyond all bounds. With regard to the variable drive parts stress it is inadmissible. Therefore we limit the in practice possible minimum ring motion value to $x_{min} = 2.8$ mm.

Table 1 and Figure 5 present summary of numerical values at extreme values of the ring motion. Values are calculated using equations (7), (9), (10), (11).

According to the manufacturer's demands the constant drive ratio of

$$\mu_{6K} = \frac{n_k}{n_{61}} = \frac{1}{5}$$

should be applied. Where n_k are the travel wheel revolutions.

From here for $x_{min} = +2.8$ mm at $n_{61} = 156$ 1/min we get the travel wheels revolutions

$$n_{kmin} = 31.2 \text{ 1/min}$$

(i.e. the first speed of small tractors). For $x_{max} = +14$ mm the travel wheels revolutions are

$$n_{max} = 141 \text{ 1/min}$$

(i.e. the third speed of small tractors).

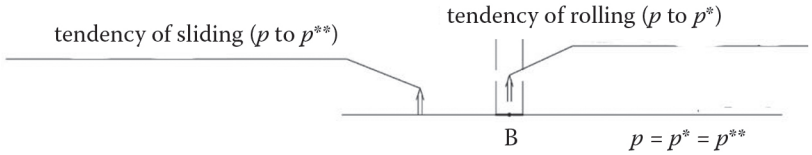

Figure 4. Simplified diagram of angles of contingency

Table 1. Limiting revolutions of single parts

	x_{min} = +2.8 mm	x_{max} = +14 mm	x_{min} = –2.8 mm	x_{max} = –14 mm
$N_{31} = n_{21}$ (1/min)	2920	2920	2920	2920
N_{41} (1/min)	–487.5	–103	–679.7	–1064
N_{56} (1/min)	–2764	–2215	–3084.8	–3849
N_{61} (1/min)	156	705	–164.8	–929.1

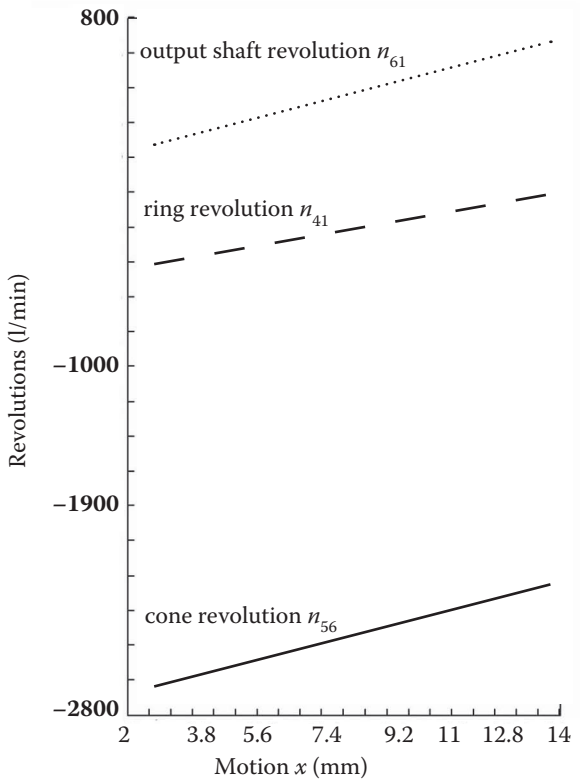

Figure 5. Relation between single parts of variable speed drives and ring motion

For positive values of the ring motion +2.8 mm ≤ x ≤ +14 mm at the constant drive ratio 1:5 the variable speed drive fulfils the by practice confirmed values of traveling speeds.

Measurement

The measurement described in this paper was intented on the verification of the real kinematical output characteristic of the variable speed drive.

The determination of the output characteristic was intented only on the output speed measuring. The determination of single internal parts revolutions is not described.

For reliability performance and theoretical premises of the mechanical variable speed drive the output characteristic determination is necessary.

In chapter 3 the mathematical relation between output speed and ring motion was derived.

The comparison of the theoretical kinematical characteristic with the real characteristic was the aim of the measuring. The measuring was carried out using the test station (Figure 6), which was placed in the laboratory of Department of Mechanics and Engineering.

The test station contains the three-phase synchronous electric motor of the power P = 4.5 kW, nominal revolutions n = 2800 1/min and the stroboscope speed meter STROBODIN.

For given test conditions the output shaft theoretical maximum and minimum speed were determined using the equation (9).

N_{min} = 156 1/min

N_{max} = 705 1/min

Using the motion shaft we adjusted approximately the central ring position and we measured the out-

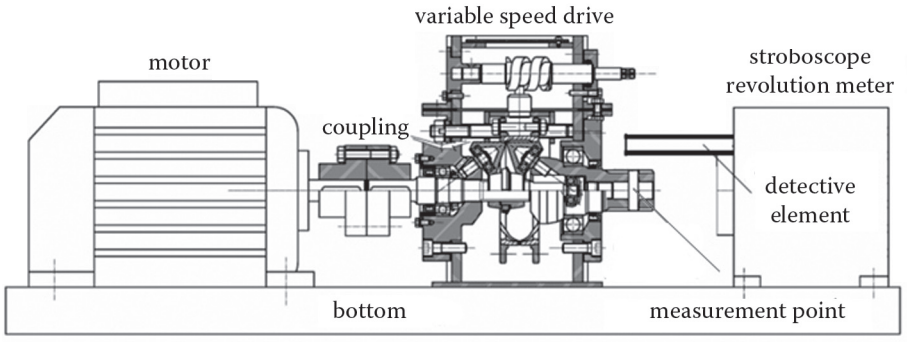

Figure 6. Arrangement of the test station – revolution measuring

Table 2. Measured values of the output speed

Motion shaft				Output shaft				
Turn of the shaft (°)	ring position (mm)		theoretical revolutions n_{61} (1/min)	measured revolutions n_{61} (1/min)				
	absolute	relative						
0	2.80	0.00	158	157	160	162	159	161
10	3.35	0.55	190	189	191	188	187	192
20	3.90	1.10	223	220	223	218	216	224
30	4.45	1.65	255	250	255	251	260	256
40	5.00	2.20	289	290	285	293	291	286
50	5.55	2.75	322	320	318	322	325	316
60	6.10	3.30	356	358	360	355	359	357
70	6.65	3.85	391	388	386	390	392	387
80	7.20	4.40	425	420	425	426	423	421
90	7.75	4.95	460	458	456	460	462	455
100	8.30	5.50	496	490	495	498	496	492
110	8.85	6.05	532	530	534	532	533	535
120	9.40	6.60	568	566	570	564	560	569
130	9.95	7.15	605	605	610	600	608	603
140	10.50	7.70	643	640	645	643	642	647
150	11.05	8.25	680	678	682	685	676	683
160	11.60	8.80	719	720	718	715	725	722
170	12.15	9.35	757	760	758	762	757	764
180	12.70	9.90	796	795	800	794	799	796
190	13.25	10.45	836	835	840	836	842	838
200	13.80	11.00	876	882	877	879	880	873

put speed. Then we moved the ring position very slow and measured the outputs speed. Reaching the minimum speed N_{min} we marked the ring position respectively the turn of the motion shaft as the minimal end point. Then we increased the output shaft speed using the motion shaft and in successive positions we measured the output shaft speed. Reaching the maximum speed we marked the ring position respectively the turn of the motion shaft as the maximal end point.

When testing the ring was positioned in the minimal point and this position was marked as the initial position, i.e. the angular rotation zero. By the next rotation always of 10° the next ring positions were determined and the output shaft speeds were measured. The measured values are presented in Table 2. For further measuring the name "relative ring motion" was introduced. This value was measured from the minimum end point, which was determined as the zero position. The absolute position corresponds to this position. It is measured from the point where the cones axes intersect.

Between both motions a simple relation is accepted

absolute position (mm) – *relative position* (mm) = = 2.8 (mm) (13)

RESULTS OF MEASUREMENTS

Output speed

Measured values of the output speed (Table 2) are presented graphically (Figure 7).

The polynomial conic curve interlayed through the measured values corresponds to the theoretical premise. The relation can be described using the regression curve

$$y = 0.6966x^2 + 53.644x + 2.812 \quad (14)$$

where y – output speed (1/min),
x – *relative* ring motion (mm)

The determination index $R^2 = 0.998$.

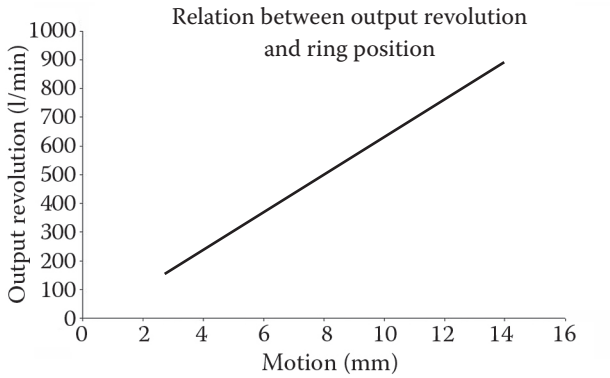

Figure 7. Output characteristic of the variable speed drive

When we introduce the geometrical data of the variable speed drive in the equation (10), which describes the theoretical relation, we get

$$n_{61} = 5600 \times \frac{x}{102 - x} \quad (15)$$

DISCUSSION

From the measured values we determined that the geometrical characteristic, i.e. relation between output speed and ring position, corresponds in the ring position range (2.8 ÷ 14) mm to the theoretical premise. We can presume that with regard to the insignificant difference between the theoretical and measured speeds the slip values of the single parts are insignificant regarding to the influence over the speed. If we represent the theoretical characteristic (15) and the real one – measured (14) we find that in the range of the ring motion the differences between individual speed values are (from –0.41 min to 0.55 min) (Figure 8). In practice these differences are irrelevant. Therefore we can presuppose that in the given ring motion range the theoretical characteristic and the measured one are identical. If we present graphically the differences between the theoretical speed (15) and the real one (14) we get the curve which shape resembles to the sine curve (Figure 9).

The curve shows in detail the behaviour of the theoretical and real speed differences (Figure 9). The distribution of the speed difference values corresponds to the sine curve with three zero points (Lorentz 1986; Mathé 1999).

CONCLUSIONS

In the present a row of simple friction, belt, chain, wave and differential variable speed drives is published. For the required range of speed variation they are altogether unfit (Amiss *et al.* 2000).

The today used power transmissions are of low efficiency (60–70%). Therefore the better power transmission efficiency is required.

The possibility of multicontact power transmission appears as the most suitable principle of the power transmission.

Using the designed function model, which was made according to the small tractor producers requirements, the real output kinematical characteristic was measured.

The real kinematical relation (relation between speed change and ring motion) corresponds to the theoretical kinematical characteristic.

All values were measured in the so-called zero operation (50 h of operation). They prove that the designed type of the mechanical variable speed drive fulfils the theoretical premises (kinematical characteristic), but it is not possible to presume the long-time operation behaviour. At present the verification of mechanical properties is carried out and the validities of measured characteristics on the operation time are verified. The output moment and the total power transmission efficiency are measured. These data are necessary for

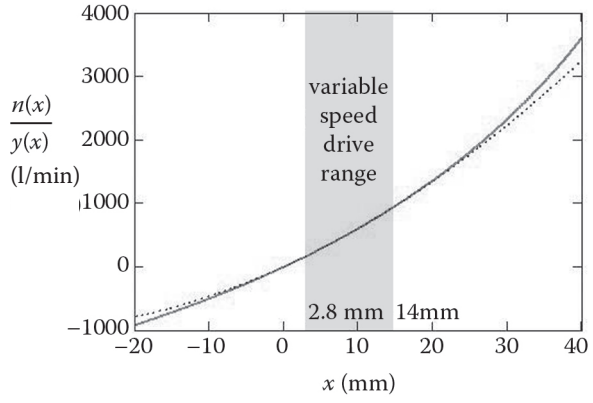

Figure 8. Relationship between theoretical and real output speed and the ring motion

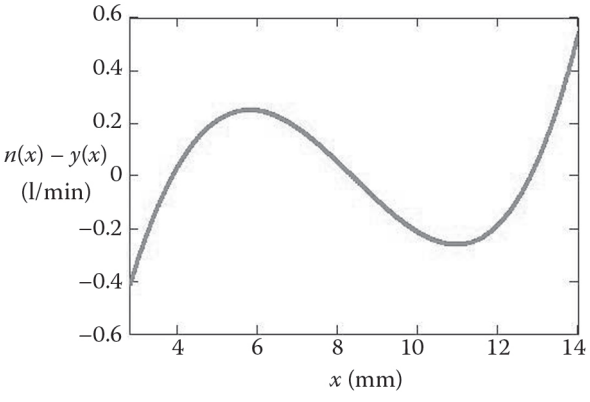

Figure 9. Relation between the difference of the theoretical and real output speeds and the ring motion

the output characteristic determination of the variable speed drive and are needful for the long-time measuring of service life characteristics.

When measuring the multiple area of natural frequency was visually determined. The natural frequency depends on many factors (constructional, industrial, operating, tribological, material etc.). From determined values the origin and the exact position of the natural frequency zone cannot be directly determined. The reasons are: the test station is determined only for the kinematical characteristic measurement, during the measurement the materials and sizes were changed, the functional model was not made precise.

Contemporary further measurements are carried out, which verify the working characteristic of the mechanical variable speed drive.

The measured values of the long-time measuring will certainly conduce to the changes in design and in materials. The changes will be directed to the better drive use efficiency.

References

Amiss J., Franclin D., Ryffel H. *et al.* (2000): Machinery's Handbook Guide. 27th Ed., Industrial Press Inc., New York.

Bolek A., Kochman J. (1989): Části strojů. Svazek 1. SNTL, Praha.

Bolek A., Kochman J. (1990): Části strojů. Svazek 2. SNTL, Praha.

Faires V.M. (1955): Design of Machine Elements. The Macmillan Company, New York.

Herák D. (2005): Mechanické variátory otáček pro přenášený výkon 0 až 50 kW. [Dizertační práce.] TF ČZU v Praze, Praha.

Kopáček J. (1997): Mechanické a hydraulické převody. VŠB – TUB, Ostrava.

Král Š. (2002): Časti a mechanizmy strojov. II. Diel. STU, Bratislava.

Lorentz G.G. (1986): Bernstein Polynomals. 2nd Ed., Chelsea Pub. Co., Chelsea.

Mathé P. (1999): Approximation of Hölder Continuous Functions by Bernstein Polynomials. American Mathematical Monthly, **106**: 568–574.

Švec V. (1999): Části a mechanismy strojů – Mechanické převody. ČVUT, Praha.

Zachariáš L. (2005): Části strojů. ČZU, Praha.

Received for publication December 14, 2005
Accepted after corrections January 3, 2006

Abstrakt

Herák D., Šleger V., Chotěborský R., Houška K., Janča E. (2006): **Kinematická charakteristika třecího mechanického variátoru otáček.** Res. Agr. Eng., **52**: 61–68.

Článek popisuje nový systém mechanického třecího sférického kuželového variátoru otáček. V současnosti je publikována řada jednoduchých třecích, řemenových, řetězových, vlnových a diferenciálních mechanických variátorů, pro požadovaný rozsah změny převodu vesměs nevhodných. Při malé účinnosti přenosu energie dosahované u současných způsobů přenosu výkonu na vývodový hřídel (60–70 %) proto vznikl požadavek lepšího využití výkonu, který dispozičně dává použitý motor. Jako nejvhodnější princip řešení je podle výzkumu prováděného autory článku využití možností vícekontaktního přenosu energie pomocí třecích sil. V článku je odvozena kompletní kinematika variátoru a popsáno sestrojení teoretické kinematické charakteristiky, která je dále porovnána se skutečnou charakteristikou zjištěnou z měření ve zkušební stanici. Z naměřených hodnot bylo zjištěno, že geometrická charakteristika, tzn. charakteristika výstupních otáček odpovídá v rozsahu posuvu prstence x = (2.8 ÷ 14) mm teoretickému předpokladu.

Klíčová slova: variátor; třecí převod; kinematická charakteristika; kinematické řešení

Corresponding author:

Ing. David Herák, Ph.D., Česká zemědělská univerzita v Praze, Technická fakulta, katedra mechaniky a strojnictví, Kamýcká 129, 165 21 Praha 6-Suchdol, Česká republika
tel.: + 420 224 383 186, fax: + 420 220 921 361, e-mail: herak@tf.czu.cz